

# EXOSIMS

## Numerical Methods for Prioritization of Exoplanet Imaging

Willard Guy Andrews IV

Daniel Jazlan Wilentz

May 24, 2017

### Contents

<b>1</b>	<b>Abstract</b>	<b>2</b>
<b>2</b>	<b>Acknowledgements</b>	<b>2</b>
<b>3</b>	<b>Motivation</b>	<b>2</b>
3.1	Development of a Program to Search for Long Term Stable Exoplanetary Orbits . . . . .	2
3.2	Maximize Efficiency of Future Imaging Missions . . . . .	3
<b>4</b>	<b>Background</b>	<b>3</b>
4.1	Current Exoplanet Orbital Information . . . . .	3
4.2	Doppler Spectroscopy . . . . .	4
4.3	Transit Photometry . . . . .	4
<b>5</b>	<b>Technical Approach</b>	<b>4</b>
5.1	Simulation Summary . . . . .	4
5.2	Data Importation . . . . .	5
5.3	Representative Test Planet Generation . . . . .	5
5.4	Semimajor Axis Bounds . . . . .	7
5.5	Simulation Initialization . . . . .	7
5.6	Equations of Motion . . . . .	7
5.7	Integrator Description . . . . .	7
5.8	Orbital Stability Criteria . . . . .	8
<b>6</b>	<b>Example Results</b>	<b>8</b>
6.1	Sample Group . . . . .	8
6.2	Simulation Results . . . . .	8
6.3	Rankings for Future Imaging . . . . .	9
6.4	Future Work . . . . .	10
<b>7</b>	<b>Appendix</b>	<b>10</b>
7.1	MATLAB Code . . . . .	10
7.2	References . . . . .	11

# 1 Abstract

The purpose of this study is to develop a program to examine the propensity of established exoplanetary systems to house additional, undiscovered exoplanets. This study is in support of NASA's WFIRST (Wide-Field Infrared Survey Telescope) mission, which is currently under development and set for a mid 2020's launch. The program in discussion will be used to formulate a series of suggestions for WFIRST operators to consider regarding where undiscovered exoplanets could be imaged. The likelihood of exoplanets existing in a given system is assessed through examining the long term stability of theoretical exoplanet orbits within that system. These orbits are obtained through Monte Carlo Simulations and are executed in MATLAB via numerical integration. This report includes the analysis and ranking of a sample population of systems to demonstrate the program's viability to be used for prioritizing future exoplanet imaging missions. Motivation, program development, and how to use the program will also be discussed.

# 2 Acknowledgements

The development of this program would not have been possible without the assistance of Professor Dmitry Savransky of the Cornell University Department of Mechanical and Aerospace Engineering. His guidance in supervising the project from both a technical and an architectural standpoint was crucial to its success. Similarly this project would not have been completed without the help of Paul West whose determined technical support shaved weeks off of development.

# 3 Motivation

## 3.1 Development of a Program to Search for Long Term Stable Exoplanetary Orbits

Studying the stability of long term orbits is the mechanism by which our team evaluates the likelihood that a system could house undiscovered exoplanets. The program focuses on single exoplanet - single star systems and operates via simulations. Given a system, each simulation uses three key steps (which can be viewed below in Figure 3.1). The first step consists of randomly generating a test exoplanet (which does not actually exist) through statistical distributions pertaining to planet mass and the 6 orbital elements (these distributions will be discussed in section 5.3). The second step involves determining the orbits of the known exoplanet and test exoplanet about their respective star through numerical integrating the orbits on a scale of one billion years (this will be discussed in detail in section 5.7). The final step pertains to studying the orbits of the exoplanets and determining if they are stable or not (stability criteria is outlined in section 5.8). These three steps comprise a single simulation. A simulation resulting in stable orbits is favorable, as it means that there is at least one situation where another exoplanet could exist in a known single exoplanet - single star system. Furthermore, if many simulations are run on a system and a large percentage of those simulations result in stable orbits, there is a significant chance that the system in question could house undiscovered exoplanets. Finally, by running many simulations on different systems, one can determine which systems are more likely to house exoplanets than others. For example, if 100 simulations are run on the 11 Ursae Minoris (11 UMi) system and on the 14 Herculis (14 Her) system each, and the 11 Umi system simulations are 27% stable while the 14 Her system simulations are only 6% stable, one can deduce that 11 Umi is more likely than 14 Her to house additional undiscovered exoplanets.

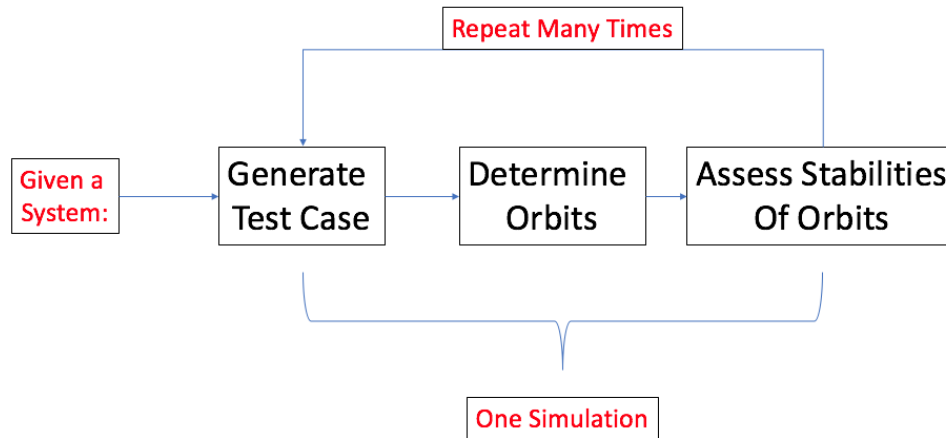


Figure 3.1: EXOSIMS Simulation Breakdown

### 3.2 Maximize Efficiency of Future Imaging Missions

By using this program to run many simulations on many different systems, one can create a list which ranks how likely single exoplanet - single star systems are to house additional exoplanets compared to one another. This list establishes favorable candidates for imaging missions and can be used by WFIRST operators to determine which single exoplanet - single star systems they should image first in the search for undiscovered exoplanets. This will allow them to optimize efficiency in future exoplanet imaging missions.

## 4 Background

### 4.1 Current Exoplanet Orbital Information

This study uses the Confirmed Planets Table on NASA's Exoplanet Archive, which is open to the public for use and can be viewed and downloaded through the URL [exoplanetarchive.ipac.caltech.edu](http://exoplanetarchive.ipac.caltech.edu) under "Data." The table currently contains information on approximately 3,500 confirmed exoplanets and is constantly growing as new exoplanets are being discovered and parametrized regularly. Some of these exoplanets are in the same system, making them multi exoplanet - single star systems. The program, in its current configuration, can run simulations on 662 exoplanets, where each exoplanet is the only currently known exoplanet in its system (making all 662 exoplanets correspond to single exoplanet - single star systems). 529 of these exoplanets were discovered with the Radial Velocity Doppler Spectroscopy method (discussed in section 4.2) while the other 133 exoplanets were discovered with the Transit Photometry method (discussed in section 4.3). These two methods have led to the vast majority of exoplanet confirmations. Direct imaging is also a substantially contributing method, but as it involves actually imaging a system, additional exoplanets in that system would have already been discovered. There are more than 662 combined Radial Velocity Doppler Spectroscopy and Transit Photometry single exoplanet - single star systems, but they are not parametrized to the extent that this program requires. In other words, there is not enough information on NASA's Exoplanet Archive to run simulations on these systems using this program. For exoplanets discovered with the Transit Photometry method, information on the exoplanet's mass and 4 of its 6 orbital parameters (semi-major axis, eccentricity, inclination, and omega) are required. For the Radial Velocity Doppler Spectroscopy method, information on the exoplanet's mass multiplied by the sin of its inclination  $m\sin(i)$ , and 3 others of its 6 orbital parameters (semi-major axis, eccentricity, and omega) are required. RAAN and mean anomaly of the known exoplanet are both set to zero for these simulations.

## 4.2 Doppler Spectroscopy

The Doppler Spectroscopy method of detecting exoplanets involves analyzing whether or not a star has wobble. Wobble is induced by a planet orbiting a star. While a planet's gravitational pull is small compared to its star's, it is not negligible. By orbiting the star, the planet will cause the star to move, ever so slightly, in a wobbling manner. A diagram of this phenomenon can be seen below in Figure 4.1

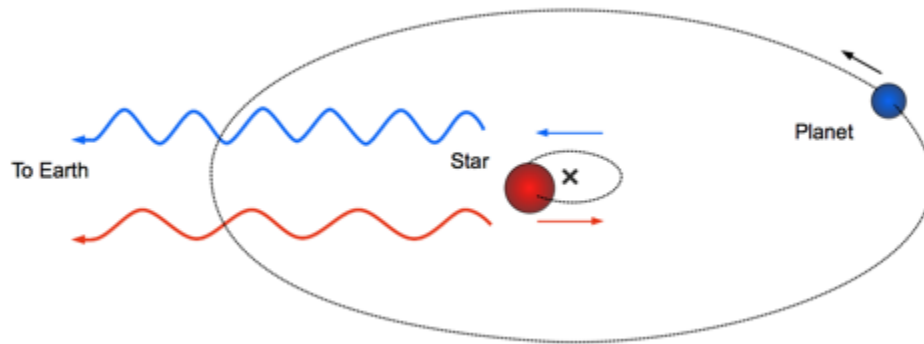


Figure 4.1: Wobble Effect

Wobble can be detected by the varying wavelengths the star emits, due to its doppler shift in moving either away from the Earth or towards the Earth based on which direction it is currently "wobbling." When the star is moving away from the earth, its wavelength will become redshifted and when it is moving towards the earth, its wavelength will become blueshifted. Therefore, if scientists observe slight but consistent changes in a star's wavelength, they can determine that the star has wobble and therefore that something must be orbiting the star. Unfortunately, this method does not allow one to determine the mass of the body orbiting the star, but rather the coupled term  $m \cdot \sin(i)$ , where  $m$  is the mass of the orbiting body and  $i$  is the body's orbital inclination. This is because observing a wobble can be due to a body orbiting in any plane except one perpendicular to the plane connecting the earth and the star (if the exoplanet was orbiting in this plane, the wobble would be perpendicular to the direction of the earth, thus creating no doppler shift towards the earth and being undetectable via this method). In situations where our team ran simulations on systems with exoplanets discovered with this method, we randomly generated the inclination, and then used that value to determine the known exoplanet's mass.

## 4.3 Transit Photometry

The Transit Photometry method of detecting exoplanets involves examining the brightness of light emitted by a given star. If an exoplanet passes directly in between its star and the earth during its orbit, the brightness of light emitted by the star will decrease. This phenomenon is much like an eclipse. Essentially, if one observes an intermittent drop in brightness from a star, one can determine that something is "eclipsing" the star and is orbiting it. This method has the advantage of providing decoupled inclination and mass information, as the exoplanet must be orbiting almost perfectly in the earth and the star's plane in order to be detected with transit photometry.

# 5 Technical Approach

## 5.1 Simulation Summary

The program SPITE (Simulation for Prioritization of Imaging of Theoretical Exoplanets) uses a monte carlo approach to determine which stars are more likely than others to contain additional, imageable exoplanets. The simulation takes in a selected group of known exoplanets to rank for future imaging in terms of the stability of orbits within their imageable regions. The number of test cases to be simulated can then be set based on the amount of computational time and power available. The bounds of the imageable regions are calculated and then

representative test cases are generated. The program then simulates the test cases for a billion years, returning the number and percentage of those test cases which were stable over the full time of simulation. The user can then rank the systems based on these percentages.

## 5.2 Data Importation

The simulation imports the classical orbital parameters from the Nasa Exoplanet Archive. The program filters the known exoplanets into two groups depending on whether true mass or  $m \sin(i)$  is known. Exoplanets without defined parameters for semimajor axis, eccentricity, omega star mass, or star distance from earth are removed from the data pool.

## 5.3 Representative Test Planet Generation

Before orbits are numerically integrated, a random planet needs to be generated. This portion of the simulation is taken care of by the function *GenerateTestCase*. This function takes as an input distance to the star in parsecs ( $d$ ) and outputs a structure which has the fields  $m$  (mass),  $e$  (eccentricity),  $i$  (inclination),  $\omega$  (argument of perigee), RAAN (Right Ascension of the Ascending Node),  $M_0$  (Initial Mean Anomaly),  $T$  (time since last anomaly), and semi-major axis ( $a$ ).  $T$  is used to calculate current mean anomaly using mean angular motion. It is always set to 0 which results in current mean anomaly also being set to 0. On the scale of one billion years, it does not matter where in its orbit the random planet starts (which is what Mean Anomaly characterizes: position of a body along its orbit).

Mass is generated according to the following probability density function (PDF):

$$p(m) = m^{-1.31}$$

The distribution will typically look like the following histogram, which was created by sampling the above PDF 2000 times:

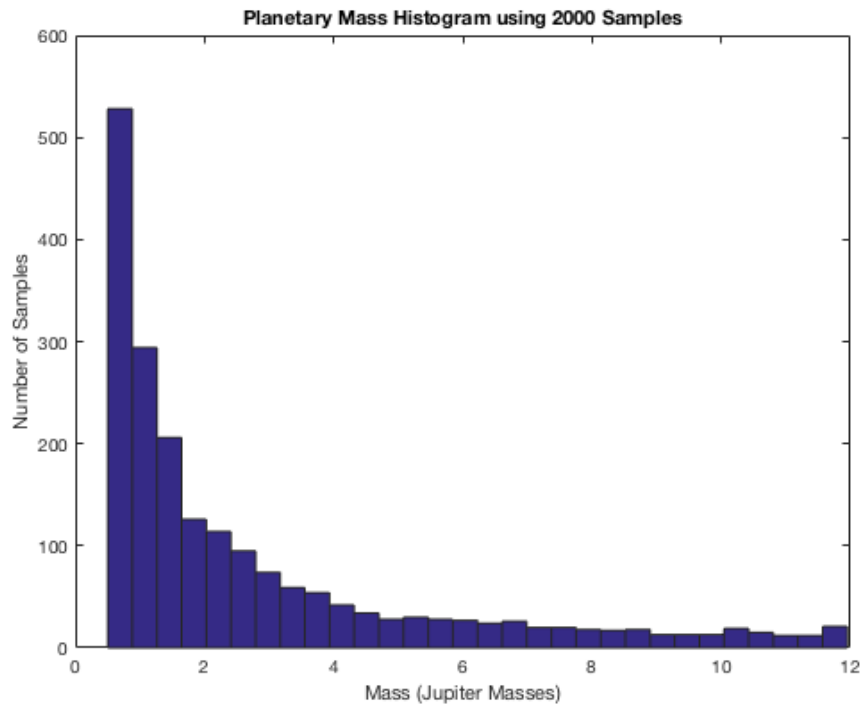


Figure 5.1: Planetary Mass Histogram

Semi-major axis is generated according to the following PDF:

$$p(a) = a^{-0.62} * e^{-2*a/S_o}$$

where  $S_o$  is set to 30 (AU). The semi-major axis distribution will typically look like the following 2000-sample histogram and will follow the distribution curve (the red dashed line). This histogram and distribution uses minimum and maximum values of 1 and 5 AU for the semi-major axis bounds (these bounds will vary for each system).

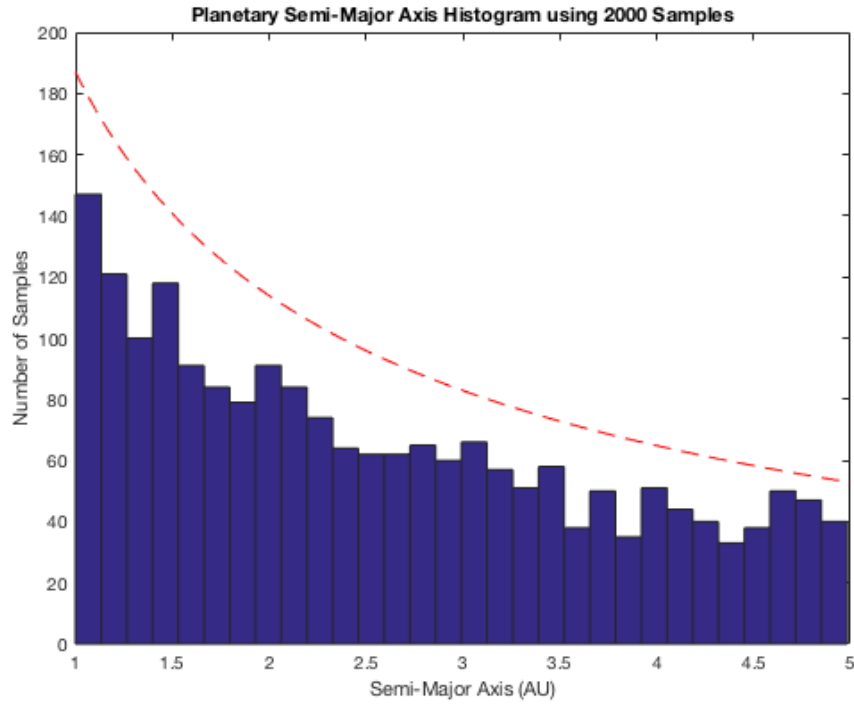


Figure 5.2: Planetary Semi-Major Axis Histogram

Specific values are ascertained from these PDFs using a sampling function *sampleDist* which was given to us by Professor Savransky. The current bounds set to mass are 0.5 and 12 (in Jupiter masses). The bounds set to semi-major axis are dependent on the distance of the system from Earth along with the mass of the planet and are created in *GenerateTestCase* by the helper function *SemiMajorAxisBouds*. The purpose of these bounds is to limit the semi-major axis to a range which can be imaged.

Eccentricity follows a Rayleigh distribution with a scale parameter of 0.21 and can be calculated with the following Matlab command:

$$e = \text{raylrnd}(0.21)$$

Inclination follows a sinusoidal distribution and can be calculated using

$$i = \text{acos}(2 * \text{rand} - 1)$$

RAAN and omega both follow uniform random distributions sized to  $2\pi$ :

$$\omega = \text{RAAN} = 2 * \pi * \text{rand}$$

This command must be called twice, once for RAAN and omega each, so that each parameter can take on a different value. If one would like to vary the planetary parameter distributions or bounds on these distributions, one should do so in *GenerateTestCase*.

## 5.4 Semimajor Axis Bounds

The bounds for generation of the semimajor axis are calculated to limit the program to the imageable region around a given star. The limit is calculated with both the geometric and optic limits of the telescope. The geometric limits are determined by the inner working angle, outer working angle, and the distance of the host star by the functions

$$a_{min} = IWA * d$$

$$a_{max} = OWA * d$$

The semimajor axis bounds are then calculated by evaluating the contrast function between the bounds calculated with the geometric limits. The contrast function is dependent on the radius of the planet, the distance from the star to the planet, the geometric albedo of the planet, and the magnitude of the phase function of the phase angle of the planet.

$$C = (r_p/r)^2 * P * \Phi(\beta)$$

$$\Phi(\beta) = \frac{\sin(\beta) + (\pi - \beta) * \cos(\beta)}{\pi}$$

$$\sin(\beta) = \frac{x^2 + y^2}{x^2 + y^2 + z^2}$$

If the contrast function is not above the detectable level for the telescope for at least 10% then the value is considered outside of the imageable space and the limit is refined. If these equations return no imageable range for a system then the simulation is forgone and the test case reported unstable as there will be no exoplanets within the non-existent imageable range.

## 5.5 Simulation Initialization

To run simulations on orbits, orbital parameters must be converted into Cartesian position and velocity vectors. This is handled by the function *InitialConditions* and the helper function *OEtoCart*. *InitialConditions* takes as inputs 3 structures corresponding to the known exoplanet, the generated exoplanet, and the star. The exoplanet structures include fields for mass and each orbital parameter and the star structure contains only one field (mass). *InitialConditions* then calls *OEtoCart* to convert these parameters into Cartesian position and velocity vectors, rearranges these vectors to be used in the numerical integrator, and outputs them.

## 5.6 Equations of Motion

The equations of motion are that of a standard 3 body problem with mutual gravitational attractive forces driving the dynamics of the system. All calculations are done in an inertial frame using Newton's Law of Universal Gravitation. Derivation of these equations is trivial and will not be covered in this report.

## 5.7 Integrator Description

Orbits are simulated using the *Rebound* software suite. The c based *Rebound* was used instead of a matlab based dynamic model because of the computational advantages of compiled machine language. Simulations run on the order of a billion years are computationally expensive. Runtime is significantly reduced by the transition from matlab's interpretive language for this section of the program. *Rebound* uses a symplectic integrator, meaning

that instead of using the first derivative of a state to determine what the new state is after a timestep, it uses the second derivative of the state. This is perfect for this program as gravitational forces are dependent only on positions and not velocities.

## 5.8 Orbital Stability Criteria

Orbital Stability is determined through two methods. The first method involves tracking how much the distances from each planetary body to the star grows over the course of the simulation. If it grows by more than a factor of 5, it is determined to be an unstable orbit. The second method involves monitoring the Kepler energy of each exoplanet. If either exoplanet's Kepler energy becomes positive, this means that this exoplanet has reached escape velocity and will leave its orbit, making it unstable. Kepler energy is defined as:

$$\varepsilon = \frac{v^2}{2} - \frac{GM}{r}$$

where  $v$  is velocity of the exoplanet,  $G$  is the gravitational constant,  $M$  is the mass of the star, and  $r$  is the distance between the star and the exoplanet. Stability checks are handled after numerical integration in the functions *ThreeBodySimMsini* and *ThreeBodySimMass*.

## 6 Example Results

### 6.1 Sample Group

The program was run for a small sample of 10 known exoplanets as a demonstration of the validity of the approach. The selected systems varied widely in terms of size, orbit, and distance from Earth.

System Number	System Name	d (Pc)	Msini (mjup)	a (AU)	e	arg of periastron (deg)	ms (mjup)
4	14 Her	18.15	4.64	2.77	0	22.6	943.1335
5	16 Cyg B	21.41	1.68	1.681	0.369	85.8	1.04E+03
15	51 Peg	15.36	0.472	0.0527	0.013	58	1.17E+03
16	6 Lyn	56.95	2.21	2.18	0.125	314.9	1.78E+03
20	7Cma	19.84	2.46	1.93	0.22	77	1.59E+03
21	70 Vir	18.11	7.4	0.481	0.399	358.8	1.14E+03
48	GJ 3021	17.62	3.37	0.49	0.511	290.7	9.43E+02
49	GJ 328	20.03	2.3	4.5	0.37	290	7.23E+02
53	GJ 433	9.04	0.018	0.058	0.08	-156	5.03E+02
79	HD 102329	138.5	5.9	2.03	0.211	182	2.04E+03

Figure 6.1: Sample Group

### 6.2 Simulation Results

50 test cases were generated and the dynamics were simulated for stability over a timespan of 1 billion years for each of the 10 selected systems. The following table displays the results of the simulations



System Number	System Name	Sims Run	Stable	Percent
4	14 Her	50	2	4
5	16 Cyg B	50	10	20
15	51 Peg	50	2	4
16	6 Lyn	50	11	22
20	7CMa	50	0	0
21	70 Vir	50	0	0
48	GJ 3021	50	0	0
49	GJ 328	50	17	34
53	GJ 433	50	35	70
79	HD 102329	50	29	58

Figure 6.2: Sample Results

Based on these results we can rank the system for future imaging priority. It may also be possible to draw conclusions about the general factors that influence stability for these systems from samples of data. GJ 433, the known exoplanet with the highest number of stable orbits is extremely small in terms of  $m \sin(i)$  and has a comparatively small semimajor axis. Comparing this result with the low percentage of stable orbits of 51 Peg, a system with nearly the same semimajor axis but an order of magnitude larger value for  $m \sin(i)$  could indicate that the known planet being small leads to a higher percentage of stable orbits. Running the program for variations on fictitious exoplanets with a single varied parameter could lead to stronger conclusions.

### 6.3 Rankings for Future Imaging

Based on the number of stable orbits found by the SPITE program the rankings for imaging of these planets would be

Ranking	System Number	System Name	Sims Run	Stable	Percent
1	53	GJ 433	50	35	70
2	79	HD 102329	50	29	58
3	49	GJ 328	50	17	34
4	16	6 Lyn	50	11	22
5	5	16 Cyg B	50	10	20
6	15	51 Peg	50	2	4
	4	14 Her	50	2	4
7	20	7CMa	50	0	0
	21	70 Vir	50	0	0
	48	GJ 3021	50	0	0

Figure 6.3: Sample Group Rankings

These results are preliminary and run with a small number of test cases. Further work should be done to evaluate the variance of the results from the program for the same systems.

## 6.4 Future Work

Conducting multiple runs with the same known exoplanets and examining the variance of the results would allow us to better define the appropriate sample size to ensure consistent results. Our current sample size was determined by restrictions on computation time and not optimized based on statistical metrics.

Running SPITE on all sufficiently parametrized systems will allow a user to create a substantial list of rankings on system propensity to house undiscovered exoplanets. SPITE should be applied to as many systems as possible to acquire useful data.

Altering SPITE to handle n-body systems rather than just 3-body systems would be helpful as it increases the number of candidate systems that can be handled. This change would allow SPITE to be applied to multiple exoplanet - single star systems and multiple exoplanet - multiple star systems.

To test SPITE's viability, it would be useful to focus on multiple exoplanet - single star systems, but treat them as single exoplanet - single star systems and see how highly ranked these systems would be to house additional exoplanets. This would be done by running the simulation as usual, but only using one of the exoplanets in the system as the known exoplanet and ignoring the others. If the program outputs a large percentage of stable simulations for these cases, this lends credence to SPITE's capability.

## 7 Appendix

### 7.1 MATLAB Code

All code and documentation on its use can be found at <https://github.com/WillardAndrews/SPITE>

## 7.2 References

Brown, Robert A. "SINGLE-VISIT PHOTOMETRIC AND OBSCURATIONAL COMPLETENESS." Space Telescope Science Institute, 7 Jan. 2005. Web.

Chambers, J. E. "A Hybrid Symplectic Integrator That Permits Close Encounters between Massive Bodies." Armagh Observatory, n.d. Web.

David A. Vallado. Fundamentals of Astrodynamics and Applications, 4th Edition. Space Technology Library. Microcosm Press, El Segundo, CA, 2013.

<http://adsabs.harvard.edu/abs/2007ARA%26A..45..397U>

<https://exoplanetarchive.ipac.caltech.edu/>

<https://exoplanets.nasa.gov/interactable/11/>

<http://iopscience.iop.org/article/10.1086/678447/pdf>

<http://iopscience.iop.org/article/10.1088/0004-637X/766/2/81/pdf>

<http://rebound.readthedocs.io/en/latest/>

<http://www.sciencedirect.com/science/article/pii/S0032063362901290>

Savransky, Dmitry, Jeremy Kasdin, and Eric Cady. "Analyzing the Designs of Planet-Finding Missions." Department of Mechanical and Aerospace Engineering, Princeton University, Princeton, 19 Mar. 2010. Web.